

---

# MAGAN: Margin Adaptation for Generative Adversarial Networks

---

Ruohan Wang Antoine Cully\* Hyung Jin Chang\* Yiannis Demiris  
Personal Robotics Laboratory, Department of Electrical and Electronic Engineering  
Imperial College London, United Kingdom  
{r.wang16, a.cully, hj.chang, y.demiris}@imperial.ac.uk

## Abstract

We propose a novel training procedure for Generative Adversarial Networks (GANs) to improve stability and performance by using an adaptive hinge loss objective function. We estimate the appropriate hinge loss margin with the expected energy of the target distribution, and derive both a principled criterion for updating the margin and an approximate convergence measure. The resulting training procedure is simple yet robust on a diverse set of datasets. We evaluate the proposed training procedure on the task of unsupervised image generation, noting both qualitative and quantitative performance improvements.

## 1 Introduction

Generative adversarial networks (GANs)[1] are generative models known for their strength at sampling from complex and intractable distributions, such as realistic image generation from natural scenes. GANs are designed as a competitive game between the generator and discriminator network, whereby the generator tries to fool the discriminator with synthetic data, while the discriminator tries to differentiate the real data from synthetic. At its theoretical optimum, the generator samples from the real data distribution. GANs have been applied to many interesting areas, including image super-resolution[2], unsupervised domain adaptation[3], driving behavior modeling[4], and synthetic data augmentation[5].

GANs are hard to train in practice. For the task of image generation, the quality of generated samples for complex domains such as natural images is still unsatisfactory, often containing visible artifacts and unrecognizable structures. More generally, GANs suffer from partial mode collapse whereby the generator only generates similar images[6] and the lack of convergence criteria[7]. Recent techniques aimed at improving GANs training, such as batch discrimination[8] and Wasserstein distance[7], often introduce new concepts in the training process, such as weight clipping, and additional hyper-parameters requiring careful tuning.

Energy-based GANs (EBGANs)[9] is a recent type of GANs that uses an auto-encoder as the discriminator. The auto-encoder aims to assign lower energy to the real data than the synthetic data. EBGANs also introduce a hinge loss objective function aimed at stabilizing the training, so that the discriminator could ignore synthetic samples with high energy. This energy margin is controlled by a hyper-parameter  $m$ . In our experiments, we observe that tuning the margin  $m$  is crucial for successful training, and that the generator loss tends to stall near the margin. A representative instance of EBGAN's stalling generator is presented in Section 3.2.

In this paper, we provide a principled analysis of the margin's effects on training and verify that the margin contributes to both stabilizing the training and stalling the generator. To address the negative effect of the margin, we propose Margin Adaptation for Generative Adversarial Network (MAGAN), that automatically sets the margin using the expected energy of the real data distribution.

---

\*These authors contributed equally to this work

The resulting training procedure is robust and stable, and produces visually appealing samples with relatively simple network architectures. We achieve improvements over the state-of-the-art results on MNIST[10], CIFAR-10[11] and CelebA[12] datasets. The procedure also provides an approximate convergence measure.

The main contributions of the paper are:

- A simple and robust training procedure that adapts the hinge loss margin based on training statistics. We remove the dependence on the margin hyper-parameter and do not introduce any new hyper-parameters to complicate training.
- A convergence measure for our proposed approach.
- A principled analysis of the effects of the hinge loss margin on auto-encoder GANs training. We observe that while the margin stabilizes the training, it also stalls the generator. This observation opens up new research directions on ways to adapt the generator/discriminator equilibrium.
- A set of experiments that demonstrate the robustness and stability of our approach, and improvements over the state-of-the-art results on a diverse set of datasets.

## 2 Related Work

Generative Adversarial Networks (GANs)[1] are a class of generative sampling models among other popular techniques such as PixelRNN[13] and Variational Auto-Encoders (VAEs)[14]. Compared to VAEs, GANs are often favored for sharper image generation. It has been shown that GANs attempt to minimize the Jensen-Shannon divergence between the real and synthetic data distribution[1].

Primary difficulties of training GANs are summarized and discussed in [6]. An important challenge is the equilibrium of the discriminator and generator as the overpowering of one network may lead to vanishing or exploding gradient, which results in training difficulties. In addition, visual inspection of generated samples are often the only practical method to estimate convergence as the objective function fluctuates during training[6, 7]. Various techniques have been proposed to improve GANs training[8, 15] to varying degrees of success. Notably, Wasserstein distance objective function[7] is used to prevent exploding/vanishing gradients, and provides the first convergence measure. Along with those advances, new concepts and hyper-parameters are also introduced, which require careful tuning and engineering to achieve best results. Our proposed method addresses primarily the equilibrium of the discriminator and generator, and the experimental results show both high quality samples and no sign of modal collapse.

Auto-encoders[16] are also extensively used in GANs training. In [15], the authors propose an auxiliary loss function such that latent features in the discriminator are matched between the real and synthetic samples using an auto-encoder. Auto-encoders are also used in Plug-and-Play Generative Networks[17] to generate realistic images at high resolution. Energy-based GAN (EBGAN)[9] uses an auto-encoder as the discriminator, which defines each sample energy using per-coordinate squared loss. Low energy samples are attributed to the data manifold. EBGAN have been shown to minimize the total variation (TV) distance between the real and synthetic data distributions[7]. The two distributions match exactly when the TV distance is zero. EBGAN introduces a hinge loss objective function to stabilize the training. The hinge loss function uses a hyper-parameter  $m$  to denote the margin (see Eq. 3), allowing the discriminator to ignore synthetic samples with energy larger than  $m$ . In practice, we observe that tuning the margin is critical for successful training, and there is no intuitive heuristics for setting the margin. Most recently, Boundary Equilibrium GAN (BEGAN)[18] extends EBGAN by proposing a loss function that matches the synthetic data energy to a fraction  $\gamma$  of the real data energy. BEGAN is related to our method as it also tracks the expected energy of real and synthetic data to balance training. BEGAN shows that the expected energy from the discriminator approximates normal distributions, and the difference in expected energy between real data and synthetic approximates Wasserstein distance. Similar to our method, BEGAN is able to generate visually pleasing and coherent samples. However, the new hyper-parameter in BEGAN forces the trade-off between generation diversity and quality, and requires a more complex training procedure, including learning rate decay and unbalanced learning rates for the two networks.

### 3 Proposed Method

We use an auto-encoder as the discriminator, and a hinge loss objective function, as was first proposed in EBGAN[9]. Though the objective function remains the same, our proposed method of adaptive margin improves the stability and performance of the training. Furthermore, our method removes the need for tuning the hinge loss margin, which is crucial for successful training.

#### 3.1 Definition

Given a data sample  $\mathbf{x} \in \mathbb{R}^{N_x}$  of dimension  $N_x$ , a generated sample  $G(\mathbf{z})$ , and  $\mathbf{z} \in \mathbb{R}^{N_z}$  of dimension  $N_z$  from a known distribution, such as Gaussian distribution  $\mathcal{N}(0, 1)$ , We define the discriminator  $D(\mathbf{x})$  and generator functions  $G(\mathbf{z})$  as follows:

$$D(\mathbf{x}) = ||Enc(Dec(\mathbf{x})) - \mathbf{x}|| \tag{1}$$

$$G(\mathbf{z}) : \mathbb{R}^{N_z} \rightarrow \mathbb{R}^{N_x} \tag{2}$$

whereby  $D(\mathbf{x})$  is a deep auto-encoder function. The discriminator loss  $L_D$  and the generator loss  $L_G$  are formally defined as:

$$L_D(\mathbf{x}, \mathbf{z}) = D(\mathbf{x}) + max(0, m - D(G(\mathbf{z}))) \tag{3}$$

$$L_G(\mathbf{z}) = D(G(\mathbf{z})) \tag{4}$$

#### 3.2 The Effects of Margin on Auto-encoder GANs Training

In our experiments with EBGAN, we observe that the expected generator loss tends to stall near the hinge loss margin, and that the improvements in visual quality of generated images become hard to identify. If we continue to train after stalling, we observe reliably that the expected energy of real data decreases while the expected energy of synthetic data increases slowly but steadily. The evolution of sample energy for both real and synthetic data during a typical EBGAN run is shown in Figure 1.

We first explain why the expected energy of the synthetic samples settles near the margin. Consider the discriminator’s loss function for each synthetic sample  $\mathbf{y} = G(\mathbf{z})$  independently, the following objective function  $f(\mathbf{y})$  is minimized:

$$f(\mathbf{y}) = p_x(\mathbf{y}) \times D(\mathbf{y}) + p_z(\mathbf{y}) \times max(0, m - D(\mathbf{y})) \tag{5}$$

whereby  $p_x(\mathbf{y}), p_z(\mathbf{y}) \in [0, 1]$ , denoting the probability of sample  $\mathbf{y}$  in the real and the synthetic data distribution respectively. During training,  $p_x(\mathbf{y}) = 0$  for  $\mathbf{y} \notin T_x$  where  $T_x$  denotes the training set of real data. For such samples, the discriminator tries to set  $D(\mathbf{y}) \geq m$  to minimize  $f(\mathbf{y})$ . Said differently, the discriminator raises the energy of any synthetic sample not exactly matching real data, regardless of how realistic they may be. The energy of  $\mathbf{y}$  fluctuates around the margin as the generator simultaneously minimize  $D(\mathbf{y})$ .

Figure 1 also shows that the discriminator continues to decrease the energy of real samples, while increasing the energy of synthetic samples, despite the generator’s effort at minimizing the energy of the synthetic samples. We hypothesize that the discriminator gradually overpowers the generator and prevents the generator from improving further. This hypothesis is aligned with the experimental results in [19], whereby adversarial examples improve the training of the discriminator and do not prevent the discriminator from converging. In particular, adversarial samples used in [19] are very similar to real samples with minimal perturbation at each pixel. They are visually indistinguishable from real samples. Yet the discriminator is able to differentiate against them during training and to converge. In contrast, synthetic samples produced by GANs often contain visible artifacts easily differentiable from real data. It is therefore difficult for the generator to produce samples not easily rejected by the discriminator, and to maintain the equilibrium between the two networks. As the training goes on, the fixed margin is unable to adapt to the changing dynamics between the discriminator and the generator, allowing the discriminator to eventually overpower the generator.

Despite the drawback of using a fixed margin, it is also an important technique for stabilizing GAN training. The margin  $m$  prevents the discriminator from wasting efforts to discriminate any samples with energy higher than  $m$ , which are likely to correspond to bad synthetic data. The discriminator is able to only focus on synthetic examples that itself believes to be sufficiently adversarial (in terms of measured energy).

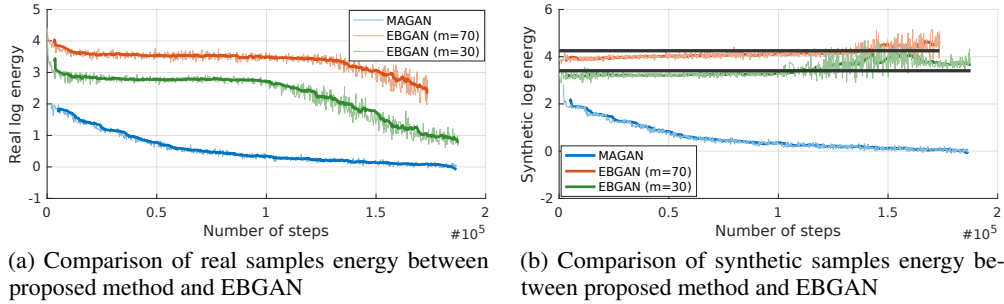


Figure 1: EBGAN(orange and green) has diverging energy for real and synthetic data, as the discriminator gradually overpowers the generator. The black line in (b) denotes EBGAN margin. The generator loss rises steadily above the preset margin. In proposed method, both real and synthetic data energy decreases in tandem. Best viewed in color.

### 3.3 The MAGAN Model

To retain the training stability that the margin provides and to allow it to adapt to the changing dynamics of the discriminator and the generator, we propose to decrease  $m$  towards the expected energy of real data. By lowering the margin from  $m_{t-1}$  to  $m_t$  where  $t$  denotes the current training epoch, the discriminator stops to differentiate against synthetic samples with energy  $m_{t-1} > D(G(\mathbf{z})) > m_t$ . Doing so, the generator is able to ‘catch up’ with the real data distribution by lowering the expected energy of synthetic samples without being simultaneously raised by the discriminator. In turn, the discriminator is presented with new adversarial examples with a different statistic that better matches the first moment of real data. The generator continues to provide high-quality adversarial samples to further the training of the both networks.

#### 3.3.1 When to Adjust the Margin

Figure 1 shows that the expected energy of synthetic data reliably increases over time with a fixed margin. One intuitive criterion is to adjust the margin at the end of a training epoch when the expected energy of synthetic data increases. We define the expected energy of real and synthetic data respectively as

$$E(D(\mathbf{x})) = \frac{1}{N_t} \sum_{i=1}^{N_t} D(\mathbf{x}^i) \quad E(D(G(\mathbf{z}))) = \frac{1}{N_t} \sum_{i=1}^{N_t} D(G(\mathbf{z}^i)) \quad (6)$$

where  $N_t$  denotes the number of real training samples. Using  $E_x^t$  and  $E_z^t$  as shorthand for the expected energy of real and synthetic data for training epoch  $t$ , the first criterion is expressed as:

$$E_z^{t-1} < E_z^t \quad (7)$$

The second criterion is to adapt the margin only when the expected energy of the real data is both below the margin  $m$  and below the expected energy of synthetic data. The second criterion captures the intuition that the discriminator should be able to firstly attribute lower energy to real data, which provides sufficient amount of samples with low energy that the generator could imitate from with gradient descent. The second criterion is defined as:

$$E_x^t < m_t \quad \text{and} \quad E_x^t < E_z^t \quad (8)$$

We combine the two criteria for a conditional update of the margin  $m_t$  at the end of each epoch. Implementation details are given in Algorithm 1. We note that by combining the two criteria, we also obtain a desirable property: the margin monotonically decreases during the training and does not oscillate.

We note that the margin adaptation based on statistics is more robust than any fixed scheduling margin update. The dynamics between the discriminator and the generator are complex and influenced by numerous factors, such as the learning rate and the network capacity. A fixed schedule is unlikely to be robust across different choices of architectures and parameters. Furthermore, the expectation of the real data distribution fluctuates during training, updating the margin with a fixed schedule may result in oscillations in the margin value as well.

---

**Algorithm 1** MAGAN algorithm. All experiments use  $\alpha = 0.0005$ ,  $b = 64$

---

**Require:**  $\alpha$ , the learning rate,  $b$ , the batch size,  $N$  the training set size,  $T_{max}$  the max number of training epochs

**Require:**  $w$ , initial discriminator parameters,  $\theta$ , initial generator parameters

```

1:  $m_0 = 0$ 
2: for  $t = 1$  to 2 do ▷ Pre-train discriminator
3:   for  $j = 1$  to  $\lfloor N/b \rfloor$  do
4:     Sample  $\{\mathbf{x}^i\}_{i=1}^b$  a batch from the real data
5:      $g_w = \nabla_w [\frac{1}{b} \sum_{i=1}^b D(\mathbf{x}^i)]$  ▷  $\mathbf{z}^i$  ignored as  $m_0 = 0$ 
6:      $w = w + \alpha \times \text{Adamax}(w, g_w)$ 
7:   end for
8: end for
9:  $m_1 = E(D(\mathbf{x})), S_z^0 = \infty$ 
10: for  $t = 1$  to  $T_{max}$  do
11:    $S_x^t = 0, S_z^t = 0$  ▷ Collect statistics into  $S$  to compute  $E$ 
12:   for  $j = 1$  to  $\lfloor N/b \rfloor$  do
13:     Sample  $\{\mathbf{x}^i\}_{i=1}^b$  a batch from the real data ▷ Train the discriminator
14:     Sample  $\{\mathbf{z}^i\}_{i=1}^b$  a batch from the prior samples
15:      $g_w = \nabla_w [\frac{1}{b} \sum_{i=1}^b (D(\mathbf{x}^i) + \max(0, m_i - D(G(\mathbf{z}^i)))]$ 
16:      $S_x^t = S_x^t + \sum_{i=1}^b D(\mathbf{x}^i)$ 
17:      $w = w + \alpha \times \text{Adamax}(w, g_w)$ 
18:     Sample  $\{\mathbf{z}^i\}_{i=1}^b$  a batch from the prior samples ▷ Train the generator
19:      $g_\theta = \nabla_\theta [\frac{1}{b} \sum_{i=1}^b D(G(\mathbf{z}^i))]$ 
20:      $\theta = \theta + \alpha \times \text{Adamax}(\theta, g_\theta)$ 
21:      $S_z^t = S_z^t + \sum_{i=1}^b D(G(\mathbf{z}^i))$ 
22:   end for
23:   if  $S_x^t/N < m_t$  and  $S_x^t < S_z^t$  and  $S_z^{t-1} < S_z^t$  then ▷ Update the margin
24:      $m_{t+1} = S_x^t/N$ 
25:   end if
26: end for

```

---

### 3.3.2 How to Set the Margin

We choose  $m_t = E_x^t$  for simplicity, which approximately guides the generator towards the real data distribution. In practice, the computation of expectation requires almost no additional resources as the expected energy of mini-batches are needed for computing gradient. In order to get an initial estimate of the margin, we briefly pre-train the discriminator with an auto-encoder objective for 2 epochs using only real samples (equivalent to setting  $m = 0$ ) and calculate the expected energy of the real data. We note that at the very early steps of training, both EBGAN and BEGAN train the discriminator largely with only real data due to their formulation of the objective functions. We also note that an advantage of auto-encoder GANs is that the discriminator can be fully pre-trained in an unsupervised way. In contrast, a classification network, the discriminator of a normal GAN, requires either a good source of negative examples or class labels for pre-training.

We hypothesize that progressively decreasing the margin as soon as the expected energy of synthetic samples increases allows the training process to control the dynamics of both the discriminator and the generator. In particular, when the expected energy of synthetic samples starts to increase, this most likely suggests that the discriminator is starting to overpower the generator. By reducing the margin at this moment to the level of the expected energy of real samples, we force the discriminator to focus only on the best (in terms of energy) synthetic samples (those that remain below the new margin) while fostering better reconstruction of real ones. Said differently, when the discriminator starts to overpower the generator, reducing the margin diminishes the pressure on the generator, allowing it to find a way to fight back, while at the same time challenging the discriminator by presenting only the best samples and making the reconstruction of the real samples a higher priority than the discrimination aspect (because most of the synthetic samples are not used to compute the loss of the discriminator). This dynamic adaption of the margin demonstrates in practice to be an effective way to keep the discriminator and generator in balance.

The concept of exploiting the expected energy of real data is also independently proposed in BEGAN[18], whereby the objective function aims to match  $E_z^t = \gamma E_x^t$  with  $\gamma$  as a hyper-parameter. We observe that our method is different in several significant ways:

- We retain the theoretical optimality of the original EBGAN by minimizing the TV distance between the real and synthetic data distributions[7]. When the TV distance equals to 0, the two distributions match exactly. In contrast, BEGAN minimizes the approximate Wasserstein distance between  $E_x^t$  and  $E_z^t$ , which in this application is not shown to match the real and synthetic distributions exactly.
- Our method does not introduce any new hyper-parameter. On the contrary, we remove the dependence on the margin hyper-parameter in the hinge loss function introduced by EBGAN.
- Our method does not force the expected energy of the synthetic data to match that of the real data, but simply guide the generator towards the expected energy of the real data.
- Our method has a simpler and more robust training procedure, with fixed and balanced learning rate for both networks. BEGAN requires a learning rate decaying schedule, and different learning rates for the two networks.

### 3.4 Convergence Measure

Until recently, GAN is known for lacking good convergence criteria as the objective function is formulated as a zero sum game, resulting in seesawing of discriminator and generator losses. Visual inspection of generated images is widely used as a practical ways to determining convergence. Wasserstein GAN[7] was the first to derive a convergence measure based on Wasserstein distance loss. We also derive a practical convergence measure based on two observations:

- The discriminator is fundamentally an auto-encoder, which would continue to reduce the energy of real data samples until saturation. Adversarial examples have been shown to even improve the training of discriminator[19].
- The hinge loss implicitly guides the energy of synthetic data towards the margin  $m$ . As we adaptively set the margin to be the expected energy of the real data, the expected energy of the synthetic data should also decrease. At its theoretical optimum, the condition  $E_x^\infty = E_z^\infty$  holds.

The convergence measure is therefore defined as:

$$L_{train} = E_x^t + |E_x^t - E_z^t| \quad (9)$$

The first term of the equation captures the observation that energy of real data distribution decreases over training, while the second term describes that at optimum, the two expectations are equal.

### 3.5 Model Architecture

We use a deep convolutional generator analogous to DCGAN’s[20] for all experiments. For discriminators, we use a fully-connected auto-encoder for MNIST dataset to prevent overfitting, and a fully convolutional one for CIFAR-10 and CelebA datasets. The convolutional auto-encoder is composed of strided convolution for encoding and fractional-strided convolutions for decoding. For convolutional discriminators, we use Leaky Rectified Linear Unit (Leaky RELU)[21] to provide dense gradients to generators, which is known for improving the results[20]. We use RELU for all other activations except for the last layer of the discriminator and generator. Sigmoid units are used for MNIST and tanh units are used for CelebA and CIFAR-10. The method requires no other techniques such as batch normalization[22], or layer-wise noises[9] to help with the training. We sample  $z$  from  $\mathcal{N}(0, 1)$  and determine  $N_z$  such that the number of parameters in the discriminator and generator are roughly equal. More details are given in Section 4. We will soon release the code on GitHub.

## 4 Experimental Results

### 4.1 General Setup

All models are trained with Adamax[23] with a fixed learning rate of 0.0005, and momentum  $\beta_1$  of 0.5, using a batch size of 64. Exact model architectures are reported separately for each dataset.

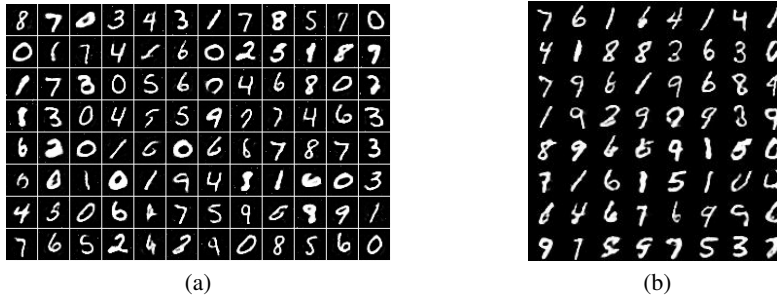


Figure 2: (a) Best MNIST generation directly taken from EBGAN-PT[9]. (b) Generation results from our methods. The generation is a single mini-batch randomly generated at the end of the training.

## 4.2 MNIST

We use a fully-connected auto-encoder for discriminator to prevent over-fitting as the dataset is relatively simple. We use 874-256-256-784 for the discriminator, whereby each number refers the unit counts in a given layer. For the generator, we set  $N_z = 50$ , to roughly balance the network capacity of the generator and the discriminator. We set the generator with the architecture (128)7c1s-(64)4c2s-(1)4c2s whereby "(64)4c2s" denotes a convolution/deconvolution layer with 64 output feature maps and kernel size 4 with stride 2. All internal activations use RELU units while the output layers of both the discriminator and the generator use sigmoid units. We compare our generation results with the EBGAN results in Figure 2. The EBGAN results are taken directly from [9]. Our results come from a single random mini-batch of samples with no manual selection.

As MNIST is a relatively simple dataset, there are no visually significant differences between our results and those of EBGAN. We observe that in our results, varying styles and orientations are present for each digit class. In addition, our method does not suffer from mode collapse with all 10 classes present in a single random mini-batch, with the count for each digit class relatively balanced.

## 4.3 CelebA

We use a convolutional auto-encoder for the discriminator, the decoder structure of the auto-encoder is used as the generator. The parameters are not shared between the discriminator and generator. The discriminator architecture is (64)4c2s-(128)4c2s-(256)4c2s-(512)4c2s-(256)4c2s-(128)4c2s-(64)4c2s-(3)4c2s. For the generator, the architecture is the decoder portion, (512)4c2s-(256)4c2s-(128)4c2s-(64)4c2s-(3)4c2s. We set  $N_z = 350$  to approximately balance the capacity of the two networks. The discriminator uses Leaky RELU for internal activations, while the generator uses RELU. The output layers of both networks use tanh units.

We again compare our generation results with the EBGAN results from [9] in Figure 3. We emphasize that the generated images come from a random mini-batch and are representative of the generator performance. No manual selection of individual images was performed.

Our method outperforms EBGAN. The images generated with MAGAN are more visually coherent, sharper and contain fewer artifacts. The background also appears to be more realistic. We note that the images are arranged in the increasing order of energy from top left to bottom right as measured by the discriminator, which suggests that within a small region of measured energy, the sample energy is not a strong indicator of 'realness' of generated images. This observation seems to contradict the training objective of BEGAN, which hypothesizes that the lower expected energy of synthetic examples correspond with better generation quality. We also note that comparison against BEGAN on face generation is not directly possible as it uses a private dataset for its experiments.

## 4.4 CIFAR-10

An architecture similar to that of the CelebA experiment is used for the CIFAR-10 experiment. The architecture of the discriminator is defined by (128)4c2s-(256)4c2s-(512)4c2s-(256)4c2s-(128)4c2s-(3)4c2s, while the generator is set as (512)4c2s-(256)4c2s-(128)4c2s-(3)4c2s. We set  $N_z = 320$ .

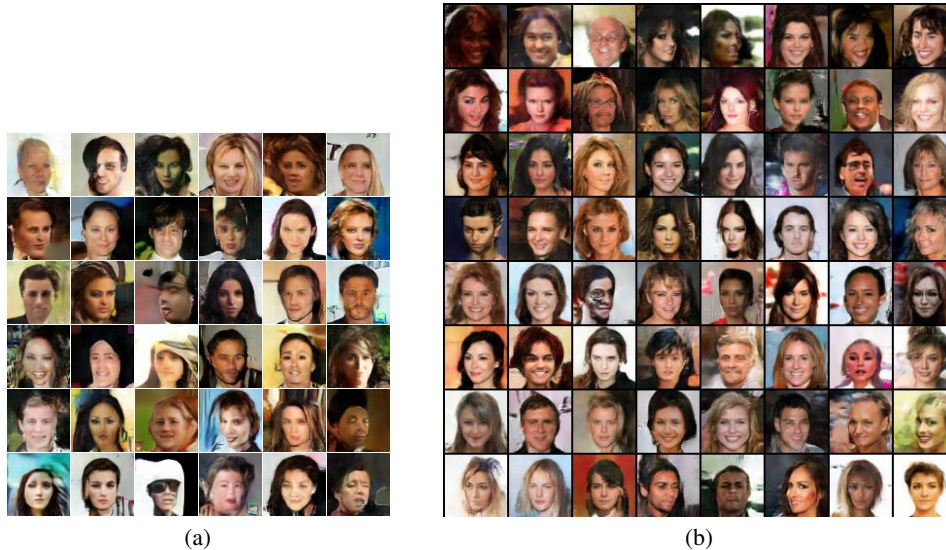


Figure 3: (a) Best CelebA generation directly taken from EBGAN-PT[9]. (b) Generation results from our methods. The generation is a single mini-batch randomly generated at the end of the training. Our results are presented such that each image is of same size as EBGAN results. Best viewed in color.

In this experiment, we quantify our results with inception score and compare against the state-of-the-art methods. The inception score is a heuristic commonly used for GANs to measure single sample quality and diversity in the inception model. The results are presented in Table 1. Similar to previously computed scores[8, 15], the inception score is calculated with 10 batches of 5000 independent samples to measure the diversity and quality of synthetic samples on a trained inception network. We use the code accompanying [8] for the computation.

With the exception of Denoising Feature Matching[15] (DFM), our method outperforms all other methods. We wish to further explore different discriminator and generator architectures to improve our results, as the small image size of CIFAR-10 poses a different challenges compared to images of higher resolution in CelebA. Further, DFM may be compatible with our framework and is a possible direction for future investigations.

#### 4.5 Convergence and Bootstrapping

In Figure 1, we show the evolution of measured energy for both the real and synthetic data during training for the MNIST experiment. We note that the figure is representative of training on all other datasets tested. We compare the energy graph against that of EBGAN (our implementation based on [26]). We set  $m = 70$  and  $m = 30$  respectively for EBGAN during two independent runs.

The results show that the expected energy of both the real data and synthetic data reliably converges to low values, while in EBGAN, the energy of real data and synthetic data diverges. As discussed in Section 3.2, the result suggests that the discriminator gradually overpowers the generator. Combined with the improved visual qualities on CelebA dataset, the results strongly suggest that using an adaptive margin effectively improves the generator performance, both in energy measure and correlated visual qualities of generated samples.

Figure 4 shows our proposed convergence measure during training on the MNIST dataset. We note that the measure is calculated at the end of the every training epoch.

Table 1: Inception score comparison

| Method                    | Score       |
|---------------------------|-------------|
| Real data                 | 11.24       |
| DFM[15]                   | 7.72        |
| BEGAN[18]                 | 5.62        |
| ALI[24]                   | 5.34        |
| Improved GANs[8]          | 4.36        |
| MIX + WGAN[25]            | 4.04        |
| <b>MAGAN (This paper)</b> | <b>5.67</b> |



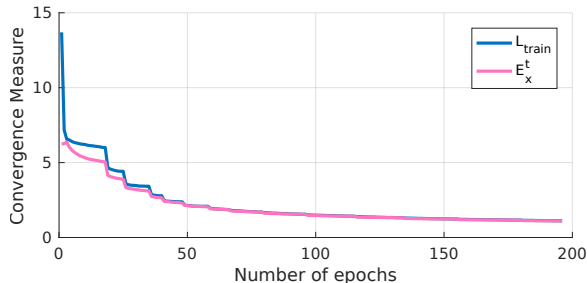


Figure 4: Our proposed convergence measure. The measure is calculated at the end of each training epoch. The pink line shows the expected energy of real samples. The difference between the two measures decreases over time

The sudden drops in the convergence measure correspond with the margin updates. The result shows that the generator is able to reduce the difference between the expected energy of the real and synthetic data until convergence.

Lastly, we show in Figure 5 the random generation results at the earliest epoch whereby they roughly resemble the shapes and textures of real data. For narrow domain datasets CelebA and MNIST, the generator converges to sensible results after a single epoch. For CIFAR-10 with diverse natural scenes, the generator takes 5 epochs to do so. The result appears to confirm the effect of the hinge loss margin in stabilizing the training, and the use of expected energy of

real samples to set the margin.

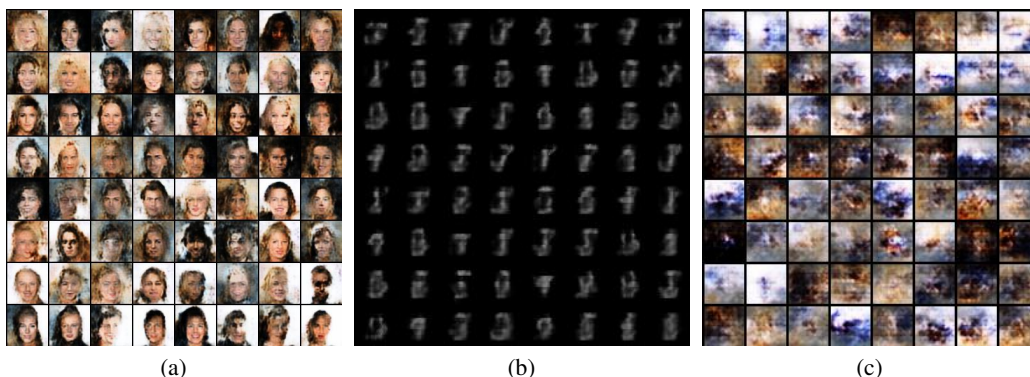


Figure 5: (a) and (b) Random mini-batch generated after 1 epoch of training for CelebA and MNIST datasets respectively. (c) Random mini-batch generated after 5 epochs of training for CIFAR-10 dataset. All generators quickly converge to sensible results.

## 5 Conclusion and Future Work

We have presented Margin Adaptation for GANs, a novel training procedure for auto-encoder GANs. We have provided an principled analysis of the hinge loss’s effects on GAN training and the experiments confirm our hypothesis that a fixed margin both stabilizes training and stalls the generator performance. The proposed method of margin adaptation overcomes the negative effect of hinge loss and achieves both qualitative and quantitative improvements, outperforming methods from the start-of-the-art. For future work, we wish to explore the use of hinge loss in other GAN frameworks to validate its general applicability. We also wish to further understand the impact of using auto-encoder as the discriminator as it appears to improve GAN training over single-output classification networks.

## References

- [1] Ian Goodfellow, Jean Pouget-Abadie, Mehdi Mirza, Bing Xu, David Warde-Farley, Sherjil Ozair, Aaron Courville, and Yoshua Bengio. Generative adversarial nets. In *Advances in neural information processing systems*, pages 2672–2680, 2014.
- [2] Christian Ledig, Lucas Theis, Ferenc Huszar, Jose Caballero, Andrew P. Aitken, Alykhan Tejani, Johannes Totz, Zehan Wang, and Wenzhe Shi. Photo-realistic single image super-resolution using a generative adversarial network. *CoRR*, abs/1609.04802, 2016.

- [3] Konstantinos Bousmalis, Nathan Silberman, David Dohan, Dumitru Erhan, and Dilip Krishnan. Unsupervised pixel-level domain adaptation with generative adversarial networks. *CoRR*, abs/1612.05424, 2016.
- [4] Alex Kuefler, Jeremy Morton, Tim Allan Wheeler, and Mykel John Kochenderfer. Imitating driver behavior with generative adversarial networks. *CoRR*, abs/1701.06699, 2017.
- [5] Ashish Shrivastava, Tomas Pfister, Oncel Tuzel, Josh Susskind, Wenda Wang, and Russ Webb. Learning from simulated and unsupervised images through adversarial training. *CoRR*, abs/1612.07828, 2016.
- [6] Ian Goodfellow. NIPS 2016 tutorial: Generative adversarial networks. *CoRR*, abs/1701.00160, 2017.
- [7] Martin Arjovsky, Soumith Chintala, and Léon Bottou. Wasserstein gan. *arXiv preprint arXiv:1701.07875*, 2017.
- [8] Tim Salimans, Ian Goodfellow, Wojciech Zaremba, Vicki Cheung, Alec Radford, and Xi Chen. Improved techniques for training gans. In *Advances in Neural Information Processing Systems*, pages 2226–2234, 2016.
- [9] Junbo Zhao, Michael Mathieu, and Yann LeCun. Energy-based generative adversarial network. *arXiv preprint arXiv:1609.03126*, 2016.
- [10] Yann LeCun and Corinna Cortes. MNIST handwritten digit database. 2010.
- [11] Alex Krizhevsky. Learning Multiple Layers of Features from Tiny Images. Master’s thesis, 2009.
- [12] Ziwei Liu, Ping Luo, Xiaogang Wang, and Xiaoou Tang. Deep learning face attributes in the wild. In *Proceedings of International Conference on Computer Vision (ICCV)*, 2015.
- [13] Aaron van den Oord, Nal Kalchbrenner, and Koray Kavukcuoglu. Pixel recurrent neural networks. *arXiv preprint arXiv:1601.06759*, 2016.
- [14] Diederik P Kingma and Max Welling. Auto-encoding variational bayes. *arXiv preprint arXiv:1312.6114*, 2013.
- [15] D Warde-Farley and Y Bengio. Improving generative adversarial networks with denoising feature matching. *International Conference on Learning Representations (ICLR)*, 8, 2017.
- [16] Pascal Vincent, Hugo Larochelle, Yoshua Bengio, and Pierre-Antoine Manzagol. Extracting and composing robust features with denoising autoencoders. In *International Conference on Machine Learning*, pages 1096–1103. ACM, 2008.
- [17] Anh Nguyen, Jason Yosinski, Yoshua Bengio, Alexey Dosovitskiy, and Jeff Clune. Plug & play generative networks: Conditional iterative generation of images in latent space. *CoRR*, abs/1612.00005, 2016.
- [18] D. Berthelot, T. Schumm, and L. Metz. BEGAN: Boundary Equilibrium Generative Adversarial Networks. *ArXiv e-prints*, March 2017.
- [19] Ian J Goodfellow, Jonathon Shlens, and Christian Szegedy. Explaining and harnessing adversarial examples. *arXiv preprint arXiv:1412.6572*, 2014.
- [20] Alec Radford, Luke Metz, and Soumith Chintala. Unsupervised representation learning with deep convolutional generative adversarial networks. *CoRR*, abs/1511.06434, 2015.
- [21] Andrew L Maas, Awni Y Hannun, and Andrew Y Ng. Rectifier nonlinearities improve neural network acoustic models. In *International Conference on Machine Learning*, volume 30, 2013.
- [22] Sergey Ioffe and Christian Szegedy. Batch normalization: Accelerating deep network training by reducing internal covariate shift. *CoRR*, abs/1502.03167, 2015.

- [23] Diederik P. Kingma and Jimmy Ba. Adam: A method for stochastic optimization. *CoRR*, abs/1412.6980, 2014.
- [24] V. Dumoulin, I. Belghazi, B. Poole, O. Mastropietro, A. Lamb, M. Arjovsky, and A. Courville. Adversarially Learned Inference. *ArXiv e-prints*, June 2016.
- [25] S. Arora, R. Ge, Y. Liang, T. Ma, and Y. Zhang. Generalization and Equilibrium in Generative Adversarial Nets (GANs). *ArXiv e-prints*, March 2017.
- [26] Namju Kim. A tensorflow implementation of Junbo et al's Energy-based generative adversarial network (EBGAN) paper. <https://github.com/buriburisuri/ebgan>, 2016.